

PAPER

## A novel antibiotic: the antimicrobial effects of CFBSA and its application on electrospun wound dressing

To cite this article: Shu Sun *et al* 2024 *Biomed. Mater.* **19** 055010

View the [article online](#) for updates and enhancements.

### You may also like

- [Electrospun vascular grafts fabricated from poly\(L-lactide-co-caprolactone\) used as a bypass for the rabbit carotid artery](#)  
Jana Horakova, Petr Mikes, David Lukas et al.
- [Promotion of adipose stem cell transplantation using GelMA hydrogel reinforced by PLCL/ADM short nanofibers](#)  
Xuchao Ning, Na Liu, Tiancai Sun et al.
- [Comparison of plasma and chemical modifications of poly-L-lactide-co-caprolactone scaffolds for heparin conjugation](#)  
Yu-Fang Hsieh, Khoren Sahagian, Fang Huang et al.



**Breath Biopsy Conference**

Join the conference to explore the **latest challenges** and advances in **breath research**, you could even **present your latest work!**

5th & 6th November  
Online

**Register now for free!**

**BREATH BIOPSY**

- Main talks
- Early career sessions
- Posters

The banner features a central circular image of a diverse group of people at a conference. To the right, three orange callout boxes with icons represent 'Main talks' (checklist icon), 'Early career sessions' (lightbulb icon), and 'Posters' (document icon). The background is dark with a subtle molecular structure pattern.

# Biomedical Materials



## PAPER

# A novel antibiotic: the antimicrobial effects of CFBSA and its application on electrospun wound dressing

RECEIVED  
15 January 2024

REVISED  
8 May 2024

ACCEPTED FOR PUBLICATION  
25 June 2024

PUBLISHED  
8 July 2024

Shu Sun<sup>1,5</sup> , Lei Cao<sup>2,5</sup>, Jinglei Wu<sup>1</sup> , Binbin Sun<sup>1</sup>, Mohamed El-Newehy<sup>3</sup> ,  
Meera Moydeen Abdulhameed<sup>3</sup>, Xiumei Mo<sup>1</sup>, Xianjin Yang<sup>4,\*</sup> and Hao Zheng<sup>1,\*</sup> 

<sup>1</sup> Shanghai Engineering Research Center of Nano-Biomaterials and Regenerative Medicine, College of Biological Science and Medical Engineering, Donghua University, Shanghai 201620, People's Republic of China

<sup>2</sup> Orthopaedic Traumatology, Trauma Center, Shanghai General Hospital, School of Medicine, Shanghai Jiao Tong University, Shanghai 201620, People's Republic of China

<sup>3</sup> Department of Chemistry, College of Science, King Saud University, PO Box 2455 Riyadh 11451, Saudi Arabia

<sup>4</sup> Key Lab for Advanced Material & Institute of Fine Chemicals, East China University of Science and Technology, Shanghai 200231, People's Republic of China

<sup>5</sup> These authors contributed equally to this work.

\* Authors to whom any correspondence should be addressed.

E-mail: [yxj@ecust.edu.cn](mailto:yxj@ecust.edu.cn) and [zhenghao@dhu.edu.cn](mailto:zhenghao@dhu.edu.cn)

**Keywords:** nitrogen-fluoride compounds, electrospinning, antimicrobial, antimicrobial mechanism, wound dressing

## Abstract

N-chloro-N-fluorobenzenesulfonylamide (CFBSA), was a novel chlorinating reagent, which exhibits potential antibacterial activities. In this study, CFBSA was confirmed as a wide-broad antimicrobial and bactericidal drug against different gram-negative bacteria, gram-positive bacteria and fungi, while it was found to have low cytotoxicity for eukaryotic cells. In addition, microorganism morphology assay and oxidative stress test was used to determine the antimicrobial mechanisms of CFBSA. According to the results, CFBSA probably had a target on cell membrane and killed microorganism by disrupting its cell membrane. Then, CFBSA was first combined with poly(L-lactide-co-caprolactone) (PLCL)/SF via electrospinning and applied in wound dressings. The characterization of different PLCL/SF of CFBSA-loaded nanofibrous mats was investigated by SEM, water contact angle, Fourier transform infrared spectroscopy, cell compatibility and antimicrobial test. CFBSA-loaded PLCL/SF nanofibrous mats showed excellent antimicrobial activities. In order to balance of the biocompatibility and antibacterial efficiency, SP-2.5 was selected as the ideal loading concentration for further application of CFBSA-loaded PLCL/SF. In conclusion, the electrospun CFBSA-loaded PLCL/SF nanofibrous mat with its broad-spectrum antimicrobial and bactericidal activity and good biocompatibility showed enormous potential for wound dressing.

## 1. Introduction

After the discovery of penicillin in the 1928, many antibiotics and antimicrobial agents were successfully invented by scientists and soon became widely used [1]. However, with the abuse of broad-spectrum antibiotics, the drug resistance of bacteria arose [2]. The resistance can be related to the intrinsic characteristics of the strains or induced by drugs through mutation or gene transfer [3]. Microorganism is constantly evolution and mutation with resistance, so researchers need to constantly develop high efficiency, low

toxicity antimicrobial agent in order to deal with increasingly serious bacterial and fungal infections.

Sulfonyl-containing compounds occupy a substantial proportion in the therapeutic drugs. Because the introduction of sulfonyl group can increase the metabolic stability of drugs to prolong the duration of action [4]. In addition, the incorporation of fluorine-containing substituents is likewise valuable in the development of antibacterial and other drugs [5]. Therefore, we attempted to design a molecule that contains both one sulfonyl group and one fluorine atom. N-Fluorobenzenesulfonimide (NFSI) is

widely used as a fluorinating reagent and the cleavage of N–F bond happen in the process of fluorination reaction. It includes one N–F bond and two sulfonyl groups. The structure of NFSI is similar with our design, but one sulfonyl group is not utilized. Therefore, we designed to replace one benzene ring with a chlorine atom owing to the disinfection of the chlorinated compounds and synthesized CFBSA.

CFBSA shows a strong reactivity of the N–Cl bond, rather than the ability of fluorination. CFBSA is a novel chlorinating reagent, which has special characteristics such as simple structure, high reactivity, easy availability, and stable storage. Besides, aminochlorination products can be afforded by reacting alkenes with CFBSA [6]. Bromination process can be achieved through a one-pot strategy using CFBSA/KBr system [7].

During the study of CFBSA, we realized that the fluorine atom was not utilized. Therefore, we changed the structure of the molecule to get the compound N-fluorobenzenesulfonamide (NFH), replacing the fluorine atom of CFBSA with hydrogen atom. We found that NFH has been synthesized by Shanghai Science Bio-pharmaceutical Co. Ltd, so we bought it from the company, comparing the biological activity of NFH with CFBSA. The different antimicrobial drugs have different antibacterial mechanisms [8]. Therefore, in the present study we also further explored the antimicrobial mechanism of the drug.

As is known to all, skin acting as the protective organ with maximum area in human body often suffers infectious caused by trauma, burns and pathological changes (diabetes, venous ulcer, bedsore). Invasive bacterial and fungal infections are serious complication of traumatic wounds, the post-traumatic infections may lead to higher rates of mortality and worse clinical outcomes [9]. In addition, wound infections will introduce inflammation, interfere with re-epithelialization and postpone wound healing [10]. However, the conventional wound dressings are not able to address the problem in clinical care.

In past years, many kinds of crude materials such as linen, honey, animal fats, and vegetables fibers have been applied for wound dressing [11, 12]. Continuous developments have led to extensive use of new bandages with improved performance. Today's wound dressing materials are usually based on synthetic polymers. However, concerned about the unsatisfactory bioactivity of synthetic polymers, researchers come to recombine synthetic polymers with some natural materials (e.g. chitosan, silk, collagen, alginate, hyaluronic acid). As a polymer, poly(L-lactide-co-caprolactone) (PLCL) exhibited good biodegradability, biocompatibility and mechanical properties [13]. It can keep stable with bioactive molecules and be use for drug delivery

applications [14]. It was reported that P(LLA-CL) combined with silk fibron (SF) material was able to promote cell growth and the scaffold had good elasticity [15, 16]. With the good performance above, P(LLA-CL)/SF could be applied in wound dressing. However, SF based materials can provide nitrogen source for infectious bacteria, which limits its application on dressing material in some ways [17].

In order to cure bacterial infection on skin wounds and stop biofilm formation on dressing material, some antibacterial agent or materials have been added [18–20]. Except for some traditional antibiotics, many kinds of antibacterial materials (e.g. silver ions, quaternary ammonium compounds or nanoparticles, or antimicrobial polymers) have been applied in wound dressing [21–23]. In particular, silver-containing materials showed good antimicrobial effect [22, 24, 25]. However, these alternative materials have either considerable adverse effect such as cytotoxicity, drug resistance or high cost [24–26]. Therefore, we were anticipant to prepare a nanofiber loaded with the new antibacterial compound as a high-performance wound dressing.

In this study, the antibacterial and antifungal activities and cytotoxicity of CFBSA were studied. The antimicrobial mechanisms of this compound were further lucubrated. As a novel broad-spectrum antibiotic, CFBSA was firstly combined with PLCL/SF via blended electrospinning and applied in wound dressing. In addition, the antibacterial activities and bioactivity of CFBSA loaded PLCL/SF nanofibrous mat were tested.

## 2. Materials

### 2.1. Materials and reagents

N-chloro-N-fluorobenzenesulfonylamide (CFBSA) can be prepared from the inexpensive Chloramine B by reacting with Selectfluor in 95% yield [8] and can be easily afforded in gram scale. The reaction was allowed to stir in water at room temperature overnight. The mixture was extracted with dichloromethane and the organic layer was dried with sodium sulfate. Solvent was removed under reduced pressure and the crude product (yellow liquid) was further purified through flash column chromatography.

Silk fibroin was extracted in our laboratory. The first step was degumming, Bombyx mori cocoons (Jiaying Silk Co., Ltd) were boiled in the boiling mix solution of 0.2% (w/v) sodium carbonate and 0.3% (w/v) sodium oleate for 1 h. Then, degummed cocoons were washed with deionized water and dried. SF solution was obtained by dissolving the degummed cocoons in 9.3 M LiBr (Kanto Chemical) solution at 60 °C for 4 h [14]. The SF solution was then dialyzed against deionized water using cellulose

acetate membrane ( $M_w$ CO: 12–14 kDa) for 3 d and freeze-dried finally.

Copolymer P(LLA-CL) (LA: CL = 50:50,  $M_w$  = 300 kDa) was purchased from DaiGang Biomaterial Co., Ltd (Jinan China). 1,1,1,3,3,3-Hexafluoro-2-propanol (HFIP) was purchased from Alfa Aesar Co. (Ward Hill, MA, USA).

## 2.2. Cell culture reagents and microorganism culture reagents

Cell culture reagents, such as Dulbecco's modified Eagle's medium (DMEM), fetal bovine serum, and trypsin were purchased from Life Technologies (Waltham, MA, USA). Microorganism culture reagents, such as LB broth, YPD broth and MH broth, were purchased from Sangon Biotech (Shanghai) Co., Ltd.

## 2.3. Cell and strains

L929 cells were obtained from the Shanghai Institute of Biochemistry and Cell Biology (SIBCB, CAS, China). All the strains we used were separately purchased from ATCC (American Type Culture Collection, USA) and CMCC (National Center for Medical Culture Collection, China).

## 3. Method

### 3.1. Antimicrobial susceptibility test

K-B paper disk diffusion in accordance with the NCCLS Standards was performed for drug susceptibility before the minimal inhibitory concentration assay. *Escherichia coli* (*E.coli*), *S. aureus* (*S.a*), *Paeruginosa* (*P.a*), *Bacillus subtilis* (*B.s*), *Stenotrophomonas maltophilia* (*S.m*) and three strains of *C.albicans* (*C.albicans* ATCC10231, CMCC(F)98 001, CMCC(F)Cla) were used for testing. Sulfadiazine (SD) which is a well-known broad-spectrum antibacterial agent used in the treatment of wound infections [27]. Fluconazole (FCZ) which is a broad-spectrum antifungal drug used in clinical [28]. Therefore, the two antibiotics SD and fluconazole were used as control drugs in the tests of antibacterial and antifungal activities, respectively. The strains were isolated and cultured to mid-log phase, respectively. Then, fresh bacterial/fungal suspensions were transferred to sterile saline and were diluted to  $10^5$  CFU  $ml^{-1}$ . The 200  $\mu$ l diluent was coating on LB/YPD agar plate, with a coated rod. Next, filter paper disk with different concentration (31.25, 62.5, 125, 250  $mg\ ml^{-1}$ ) of CFBSA (dissolve in dichloromethane) were posted on the plain agar plate and the blank filter paper disk was set as negative control (0  $mg\ ml^{-1}$ , pure dichloromethane solvent). All the Petri dishes were incubated at 37 °C/28 °C for 24 h. At last, agar plates were taken out and photographed and measured the diameter of the inhibition zone, and the results were calculated as follows:

Inhibition rate (%)

$$= \frac{\text{Inhibition diameter} - \text{Paper disk diameter}}{\text{Paper disk diameter}} \times 100\%.$$

### 3.2. Minimum incubator concentration test (MICs)

The MIC is defined as the lowest concentration that inhibits over 90% of bacteria growth [29]. To make sure MIC of compound CFBSA against different kinds of microbes, micro-broth dilution was used. Besides, the SD/fluconazole was tested as positive control drug against bacterial/fungi. As the synergism assays with K-B paper disk diffusion, strains above were used for testing. Purified strains above were used for testing. *E.coli*, *P.aeruginosa*, *Bacillus subtilis*, *S. maltophilia* and *S. aureus* were cultured on LB broth plates at 37 °C for 16 h, while the fungi were cultured on PDA broth at 28 °C for 12 h with shaking at 180 rpm until reaching mid-log phase. Next, 10  $\mu$ l of fresh bacterial/fungal suspension was transferred to 10 ml of fresh MH broth/RPMI 1640 and diluted to  $10^5$  CFU  $ml^{-1}$ , then added 100  $\mu$ l into each well at 96 well and incubated at 37 °C/28 °C for 24 h. Sterilized (filter sterilization) pure CFBSA was added in the second well in each row, while the first row was set as blank control with fresh MH broth/RPMI 1640 and the last row was set as negative control. Doubling dilution was used to dilute CFBSA in 96 well, keeping concentrations of CFBSA ranging from 390.625–25 000  $\mu$ g  $ml^{-1}$ , and the mixtures were incubated at 37 °C/28 °C with no shaking for 24 h and 48 h. At last, measure the OD value at 600 nm, respectively. The experiments were performed in triplicate, and the results were calculated as follows:

Inhibition rate (%)

$$= \frac{OD\ value_{control} - OD\ value_{experiment}}{OD\ value_{control}} \times 100\%.$$

Subsequently, MIC was determined as the lowest concentration of tested drug that inhibits over 90% of bacteria growth.

After MIC test, 100 ml of each suspension was transferred onto LB agar plates or YPD agar plates and incubated at 37 °C/28 °C for 24 h. Colony enumeration was implemented after 24 h. The MBC was obtained as the lowest concentration of compound at which no colonies grew on solid medium.

### 3.3. MTT assay for cytotoxicity

In purpose of examining the cytotoxicity against L929 (normal mouse fibroblast) cells of the new compound, 3-(4,5-dimethylthiazolyl-2)-2,5-diphenyltetrazolium bromide (MTT) assay was adopted [29]. The cell treatment and infection steps in this assay were similar to those in the MIC assay. After inoculating the inoculated L929 cells in 96 well for 1 d, CFBSA was added to the second well in each row. Doubling dilution was used to dilute CFBSA in 96 well, keeping concentrations of CFBSA ranging

from 390.625–25 000  $\mu\text{g ml}^{-1}$ , and the mixtures were incubated at 37 °C with no shaking for 24 h. After that, the old medium was discarded, cleaned with PBS twice, and the serum-free DMEM medium 90  $\mu\text{l}$  was added. 10  $\mu\text{l}$  MTT solution (5 mg  $\text{ml}^{-1}$ ) was added in the dark (MTT was easily decomposed by light). Then, incubated in 37 °C for 4 h, and carefully absorbed the culture medium, 100  $\mu\text{l}$  dimethyl sulfoxide (DMSO) were added to each well. After incubating at 37 °C with shaking at 100 rpm for 30 min, the murrey crystal was dissolved and the OD values at 490 nm were measured by using a microplate reader (Multiskan MK3, Thermo, USA).

$\text{IC}_{50}$  (the half maximal inhibitory concentration) was usually used as a measure of drug toxicity. The inhibitory rate of L929 cells was calculated as follows:

$$\text{Inhibition rate (\%)} = \frac{\text{OD value}_{\text{control}} - \text{OD value}_{\text{experiment}}}{\text{OD value}_{\text{control}}} \times 100\%.$$

Then  $\text{IC}_{50}$  value was calculated by IBM SPSS Statistics. Student's t-test was performed for statistical analysis.

### 3.4. Microorganism morphology assay

*E.coli*, *S.aureus* and *C.albicans* ATCC10231 were selected as representative strains in this and subsequent experiments. Untreated bacterial/fungal samples and treated samples with half MIC concentration were obtained in a similar way to those in the live/dead bacterial assay. After 4–6 h of fixation with 2.5% glutaraldehyde, the microbes were washed three times with PBS and dehydrated with a graded ethanol series (20%–100%) for 10 min each time, then dried naturally. The samples were coated with gold and imaged with SEM at an operating voltage of 5 kV. Then, the length of bacterial/fungal before and after treatment was measured using Image J software ( $n = 20$ ).

### 3.5. Measuring of oxidative stress

The levels of malondialdehyde (MDA) and superoxide dismutase (SOD) commonly showed the level of cell oxidative stress [30, 31]. The gram-positive, gram-negative and fungal organisms MDA levels after CFBSA treated for 3 h were determined after centrifugation and in accordance with the method described by Jain [32]. The MDA content was measured according to the trichloroacetic acid method and calculated using the Hodges' equations [33]. Differently, lywallzyme was used for decomposing *C.albicans* cell wall in the two experiments. The activity of SOD was determined using a SOD assay kit (A001-1, Nanjing JianCheng Bioengineering Institute, China) according to the provided instructions and procedures.

### 3.6. Fabrication of the CFBSA loaded PLCL/SF nanofiber membrane

Firstly, P(LLA-CL) and silk fibroin respectively dissolved in 1,1,1,3,3,3-Hexafluoro-2-propanol (HFIP) at the concentration of the 10% (w/v) and 2.5% (w/v). Then, the solution was sealed and stirred at room temperature for 6 h until it is transparent. Later, add 1%, 2.5%, 5%, 10% (v/v) CFBSA (light yellow liquid) into the electron-spinning solution individually. Finally stirred and ultrasounded until all the system was thoroughly incorporated.

In brief, electrospinning solution above was placed in 10 mL plastic syringes loaded in syringe pumps (789 100 C, Cole-Parmer Instruments, USA) and operated at the rate of 0.9  $\text{ml h}^{-1}$ . The electrospinning solution in a syringe equipped with a 21 G steel needle was electrospun, using a voltage of 12 kV high-voltage power supply (BGG6-358, BMEI Co. Ltd, China). Aluminum foil (10  $\times$  10  $\text{cm}^2$ ) was used as a collector, and the distance between needle and collector was 10–13 cm. The process of electrospinning was under room temperature, and the ambient humidity is not more than 50%. The solvent which remained in nanofibrous mat was removed by vacuum drying overnight. Then the nanofibrous mat was cross-linked with glutaraldehyde vapor for 1 h and placed in fuming cupboard overnight to remove the residual aldehydet. The treated nanofibrous mat was stored in the refrigerator at 4 °C, keeping away from moisture.

### 3.7. Surface characterizations of CFBSA loaded PLCL/SF nanofiber

The surface morphology of the CFBSA loaded PLCL/SF nanofibrous mat was observed using scanning electronic microscopy (SEM). Mean fiber diameter and the distribution of fiber diameter was determined by counting 100 fibers from obtained images using Image-J software. To prove the hydrophilic and hydrophobic properties of the material, the water contact angles of nanofibrous mats were measured three times for each sample using contact angle tester (OCA40, Dataphysics, Germany).

### 3.8. Fourier transform infrared spectroscopy

In order to determine whether the compound CFBSA was successfully loaded into the nanofibers, the drug-loaded nanofiber membrane constituents and chemical structure were analyzed by Fourier transform infrared spectroscopy (FTIR). The FTIR spectra of pure CFBSA, SP-1, SP-2.5, SP-5, SP-10, and Pure SP were tested using the potassium bromide compression method. Six sets of samples were tested using attenuated total reflection (ATR) Fourier transform infrared spectroscopy (Nicolet 6700, USA). The resolution of the instrument was 16  $\text{cm}^{-1}$ , the number of scans was 128, and the scanning range was 400  $\text{cm}^{-1}$ –4000  $\text{cm}^{-1}$ .

### 3.9. Antimicrobial assessment of CFBSA loaded nanofibrous mat

To evaluate antimicrobial effect of different drug-loading rate nanofibrous mat, the diameter of inhibition zone against pathogenic strains was measured. Three typical strains *E. coli*, *S. aureus* and *C. albicans* ATCC10231 were chosen. Samples were made into circles with diameter at 13 mm and uniform thickness, using a hole puncher. Next, these samples were sterilized by ethylene oxide. The strains were isolated and cultured to mid-log phase, respectively. Then, fresh bacterial/fungal suspension was transferred to sterile saline and were diluted to  $10^5$  CFU ml<sup>-1</sup>. The 200 µl diluent was coating on LB/YPD agar plate. Next, drug loaded groups were posted on the plain agar plate and the pure PLCL/SF mat was set as negative control. All the Petri dishes were incubated at 37 °C/28 °C for 24 h. At last, agar plates were taken out and photographed and measured the diameter of the inhibition zone. And the inhibition rate was calculated as follows:

$$\text{Inhibition rate (\%)} = \frac{\text{Inhibition diameter} - \text{Mat diameter}}{\text{Mat diameter}} \times 100\%.$$

### 3.10. L929 cells proliferation on CFBSA loaded nanofibrous mat

In order to analyze the cytocompatibility of CFBSA loaded nanofibrous mat and choose the better drug-loading rate, L929 cells were cultured on them. L929 cells were cultured in DMEM with 10 wt% fetal bovine serum and 1 wt% antibiotic-antimycotic (100 units ml<sup>-1</sup> penicillin and 100 units ml<sup>-1</sup> streptomycin). The temperature and CO<sub>2</sub> concentration of the cell incubator was set to 37 °C and 5%. The DMEM medium was refreshed every two days. Samples were treated into circles and sterilized as before. L929 cells were seeded on the nanofibrous mat in 24-well plates at a density of  $1 \times 10^4$  cells per well. A cell counting Kit-8 (CCK-8) assay was conducted after culturing for 1d, 3d and 5d. In brief, the cells on the scaffolds were incubated with 360 ml RPMI-1640 and 40 ml CCK-8 for 2 h in an incubator. After that, 100 ml of the solution was transferred into a 96-well plate and the absorbance was measured by a microplate reader (Multiskan MK3, Thermo, USA) under 450 nm absorption wavelength.

### 3.11. Statistics

All experiments were performed in triplicate, and data are presented as the means  $\pm$  SD. One-way ANOVA with Bonferroni test was performed to determine the statistical significance between controls and indicated groups.

## 4. Results and discussion

### 4.1. The antibacterial activity of CFBSA

As shown in figure 1, after agar plate culture for 24 h, the inhibition rates of *E. coli*, *Stenotrophomonas maltophilia* (*S.m*), *S. aureus* (*S.a*), *Pseudomonas aeruginosa* (*P.a*) and *Bacillus subtilis* (*B.s*) were  $513.0 \pm 15.3\%$ ,  $358.1 \pm 26.6\%$ ,  $173.6 \pm 9.6\%$ ,  $298.6 \pm 13.1\%$  and  $471.2 \pm 47.1\%$ . The results indicated that CFBSA has a broad-spectrum antimicrobial activity. Moreover, there was no obvious decrease between these inhibition rate of *E.coil*, *S.m*, *S.a* and *B.s* after 24 h and 48 h. This demonstrated that the broad-spectrum bactericidal activity of CFBSA was persistent. In addition, Statistical results showed that for *E.coil*, *S.a*, *P.a*, and *B.s*, the inhibition rates of NFH and SD at the same concentrations were significantly lower than those of CFBSA ( $P < 0.05$ ). This suggests that by comparing the antibacterial activity of other compounds, CFBSA has a more sensitive antimicrobial effect against *E.coli*, *S.a*, *P.a* and *B.s* strains. Moreover, it is worth noting that CFBSA exhibited a strong antibacterial effect against *P.a*, but this strain was not susceptible to SD.

MIC is referred to the lowest concentration which limits most microbial growth, while the MBC is defined as the lowest concentration that can completely kill the bacteria. The value of MIC and MBC are obligate evaluating indicator of antimicrobial activity of CFBSA. The MIC values of CFBSA against five bacteria are listed on table 1. The MIC of CFBSA was 3125 µg ml<sup>-1</sup> for *E.coli*, 195.3 µg ml<sup>-1</sup> for *S.m*, 781.3 µg ml<sup>-1</sup> for *S.a*, 781.3 µg ml<sup>-1</sup> for *P.a* and 6250 µg ml<sup>-1</sup> for *B.s*. The MBC of CFBSA was 3125 µg ml<sup>-1</sup> for *E.coli*, 390.6 µg ml<sup>-1</sup> for *S.m*, 195.3 µg ml<sup>-1</sup> for *S.a*, 781.3 µg ml<sup>-1</sup> for *P.a* and 6250 µg ml<sup>-1</sup> for *B.s*. The MIC of NFH was 3125 µg ml<sup>-1</sup> for *E.coli* and *B.s*, 195.3 µg ml<sup>-1</sup> for *S.m*, 781.3 µg ml<sup>-1</sup> for *S.a*, and 1562.6 µg ml<sup>-1</sup> for *P.a*. The MBC of NFH was 3125 µg ml<sup>-1</sup> for *E.coli*, 390.6 µg ml<sup>-1</sup> for *S.m*, 1562.5 µg ml<sup>-1</sup> for *S.a*, 1562.5 µg ml<sup>-1</sup> for *P.a* and 3125 µg ml<sup>-1</sup> for *B.s*. The MIC of positive control drug SD was 800 µg ml<sup>-1</sup> for *E.coli* and *P.a*, 400 µg ml<sup>-1</sup> for *S.m*, 200 µg ml<sup>-1</sup> for *S.a* and 50 µg ml<sup>-1</sup> for *B.s*. Whereas, SD did not exhibit any bactericidal activity, and there were still innumerable bacterial colonies on agar plate in test of MBC.

Above all, we can make a conclude that CFBSA owes an equal antibacterial efficiency with SD against some strains and predominate activities on some drug-resistance strains (*P.a* and *S.a*). Although some MIC values of SD were smaller than CFBSA, SD are unable to kill bacteria and CFBSA has an excellent and wide-broad bactericidal property. Comparing with NFH, CFBSA has a better antibacterial and

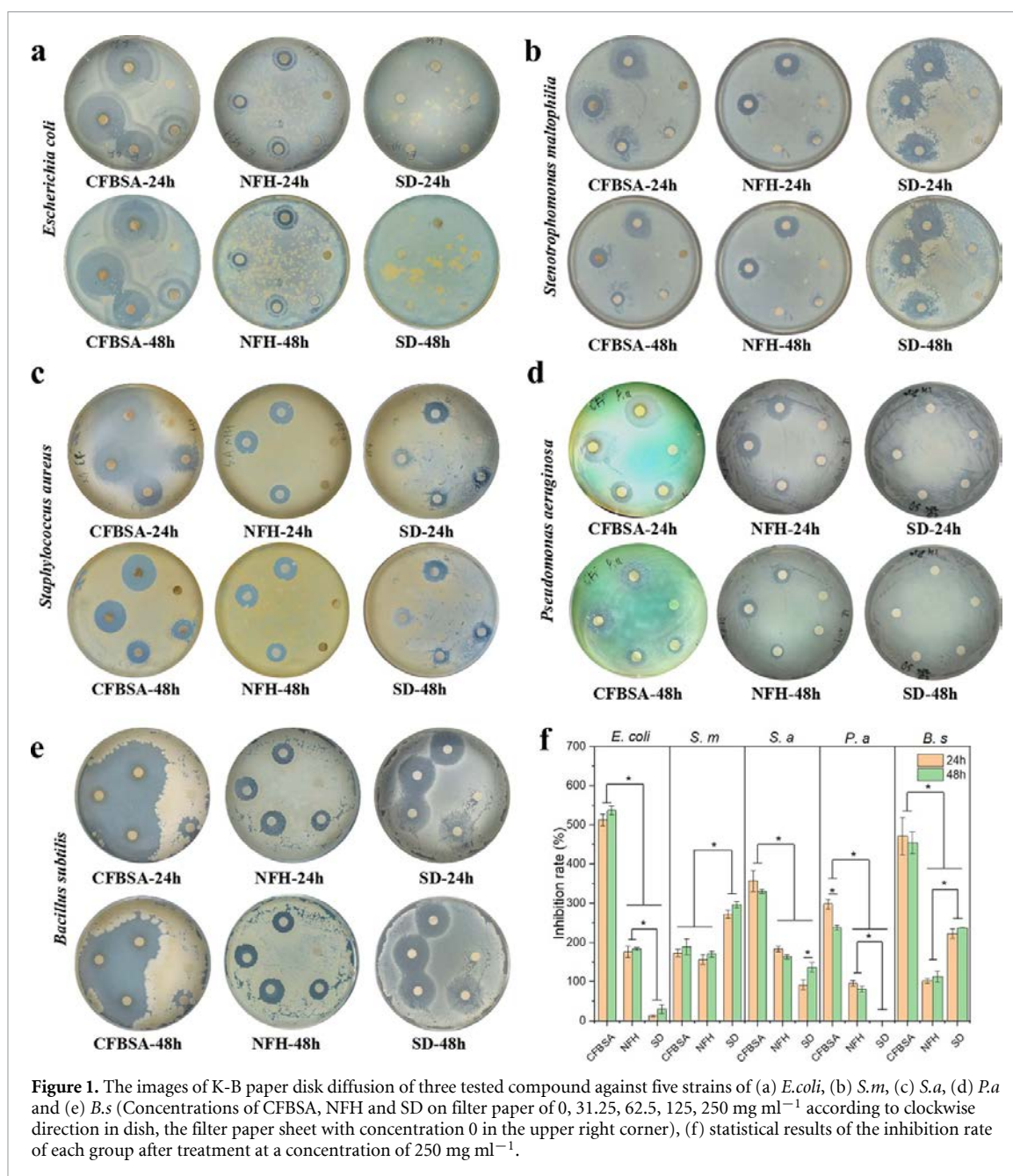


**Figure 1.** The images of K-B paper disk diffusion of three tested compound against five strains of (a) *E.coli*, (b) *S.m*, (c) *S.a*, (d) *P.a* and (e) *B.s* (Concentrations of CFBSA, NFH and SD on filter paper of 0, 31.25, 62.5, 125, 250 mg ml<sup>-1</sup> according to clockwise direction in dish, the filter paper sheet with concentration 0 in the upper right corner), (f) statistical results of the inhibition rate of each group after treatment at a concentration of 250 mg ml<sup>-1</sup>.

**Table 1.** The antimicrobial and bactericidal activity of three tested compound against gram-negative, gram-positive bacteria.

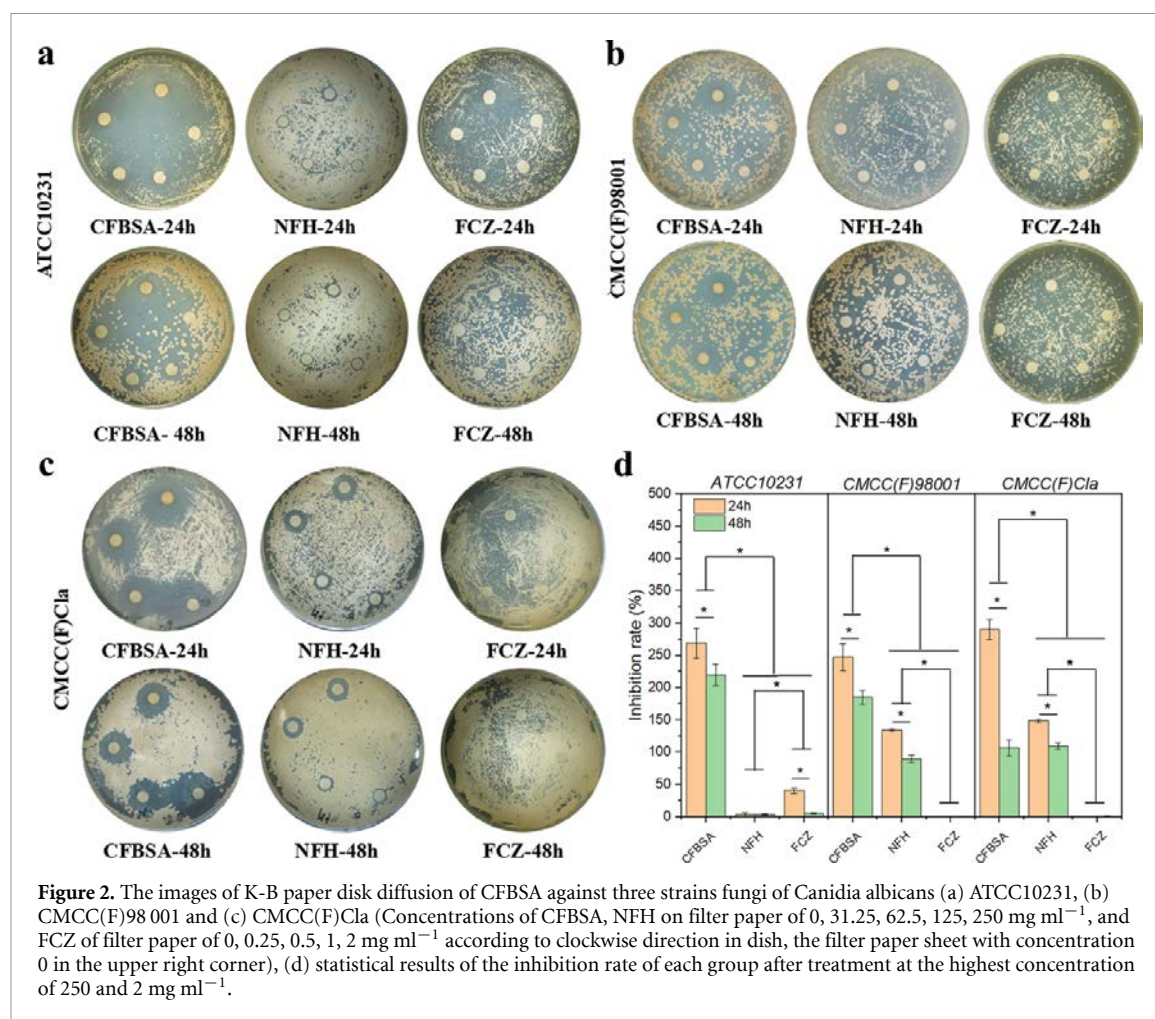
Strains	MIC/MBC ( $\mu\text{g ml}^{-1}$ )			
	CFBSA	NFH	SD	
Gram-negative	<i>E.coli</i>	3125/3125	3125/3125	800/U
	<i>S.m</i>	195.3/390.6	195.3/390.6	400/U
Gram-positive	<i>S.a</i>	195.3/195.3	781.25/1562.5	200/U
	<i>P.a</i>	781.3/781.3	1562.5/1562.5	800/U
	<i>B.s</i>	6250/6250	3125/3125	50/U

MIC: minimum inhibitory concentration, MBC: minimum bactericidal concentration, SD: sulfadiazine, U: unable to kill bacteria.

bactericidal activity, suggesting the -Cl of CFBSA contributing to its antimicrobial activity. In short, CFBSA proved as an effective and wide-broad antimicrobial drug with bactericidal activity.

#### 4.2. The antifungal activity of CFBSA

As it is shown in figure 2, after agar plate culturing for 24 h, the inhibition rate of the drug concentration of 250 mg ml<sup>-1</sup> CFBSA against



*Canidia albicans* ATCC10231, CMCC(F)98001 and CMCC(F)Cla were  $269.2 \pm 23.2\%$ ,  $247.5 \pm 20.8$  and  $290.3 \pm 15.6\%$ . After culturing for 48 h, although its inhibition rate was reduced compared to 24 h ( $249.5 \pm 17.1\%$ ,  $185.0 \pm 10.4\%$  and  $106.7 \pm 12.7\%$ , respectively), the antifungal effect could still be maintained. This demonstrated that CFBSA might owe broad-spectrum bactericidal activity. From figure 2, it can be observed that the inhibition circle diameters of NFH (250 mg ml<sup>-1</sup>) for *Canidia albicans* CMCC(F)98001 and CMCC(F)Cla, the inhibition rate of NFH of 24 h were  $134.2 \pm 1.9\%$  and  $148.8 \pm 2.2\%$ . After 48 h the inhibition rate of NFH were  $89.6 \pm 6.1\%$  and  $109.4 \pm 5.1\%$ . However, NFH had no evident inhibition area against *Canidia albicans* ATCC1023. By comparing the antibacterial activity of two compounds, CFBSA was found to have better antibacterial activity and broader antibacterial spectrum (particularly *E.coli* and *P. aeruginosa*) than SD. Besides, CFBSA also owed excellent sterilization effect, which makes it a wider application. Antifungal activity of fluconazole against three bacterial strains was shown in figure 2, 24 h after drug concentration of 250 mg ml<sup>-1</sup> of inhibition rate of fluconazole against *Canidia albicans* ATCC10231 was

$40.4 \pm 4.5\%$ , but after 48 h it is not obvious. It shows that *Canidia albicans* ATCC10231 was susceptible to fluconazole, *Canidia albicans* CMCC(F)98001 and CMCC(F)Cla were not susceptible to fluconazole.

The value of MIC and MBC are obligate evaluating indicator of antimicrobial activity of CFBSA. The MIC values of CFBSA against five bacteria and three fungi are listed on table 2. The MIC of CFBSA for *Canidia albicans* ATCC10231 and CMCC(F)98001 was  $781.3 \mu\text{g ml}^{-1}$ , and  $3125 \mu\text{g ml}^{-1}$  for *Canidia albicans* CMCC(F)Cla. And the MBC of CFBSA for ATCC10231 and CMCC(F)98001 was  $1562.6 \mu\text{g ml}^{-1}$  and for *Canidia albicans* CMCC(F)Cla was  $3125 \mu\text{g ml}^{-1}$ . And the MBC of NFH for *Canidia albicans* ATCC10231 was  $12500 \mu\text{g ml}^{-1}$  CMCC(F)98001 was  $6250 \mu\text{g ml}^{-1}$  and for *Canidia albicans* CMCC(F)Cla was  $25000 \mu\text{g ml}^{-1}$ . The MIC of NFH for *Canidia albicans* ATCC10231 and CMCC(F)98001 was  $6.25 \mu\text{g ml}^{-1}$ , and  $3125 \mu\text{g ml}^{-1}$  for *Canidia albicans* CMCC(F)Cla. As positive control, the MIC of fluconazole (FCZ) for *Canidia albicans* ATCC10231 and CMCC(F)98001 was  $6.25 \mu\text{g ml}^{-1}$  and  $0.05 \mu\text{g ml}^{-1}$  for *Canidia albicans* CMCC(F)Cla. Whereas, fluconazole did not exhibit any fungicidal

**Table 2.** The antimicrobial and bactericidal activity of three tested compound against fungi.

Strains	MIC/MBC ( $\mu\text{g mL}^{-1}$ )		
	CFBSA	NFH	FCZ
Fungi			
ATCC10231	781.3/1562.6	6250/12 500	0.625/U
CMCC(F)98 001	781.3/1562.6	6250/6250	0.625/U
CMCC(F)Cla	3125/3125	3125/25 000	0.05/U

MIC, minimum inhibitory concentration; MBC, minimum bactericidal concentration; FCZ, fluconazole; U, unable to kill bacteria.

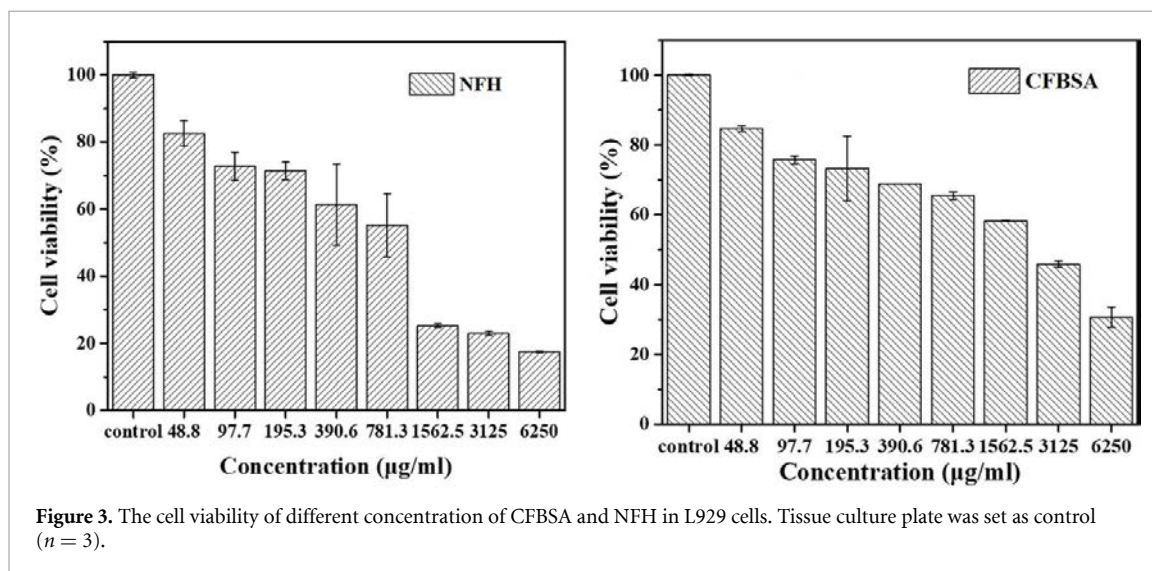


**Figure 3.** The cell viability of different concentration of CFBSA and NFH in L929 cells. Tissue culture plate was set as control ( $n = 3$ ).

activity, and there were still innumerable fungal colonies on agar plate in test of MBC.

Although some MIC values of control drugs were smaller than CFBSA, fluconazole are unable to kill fungi, while CFBSA has an excellent and better wide-broad fungicidal property. Comparing with NFH, CFBSA has a better antifungal and fungicidal activity, suggesting the -Cl of CFBSA contributing to its antimicrobial activity. As a result, cooperating with results of antibacterial test, CFBSA proved as an effective and wide-broad antimicrobial drug with bactericidal/fungicidal activity, and it is not easy for it to induce the production of drug-resistant bacteria.

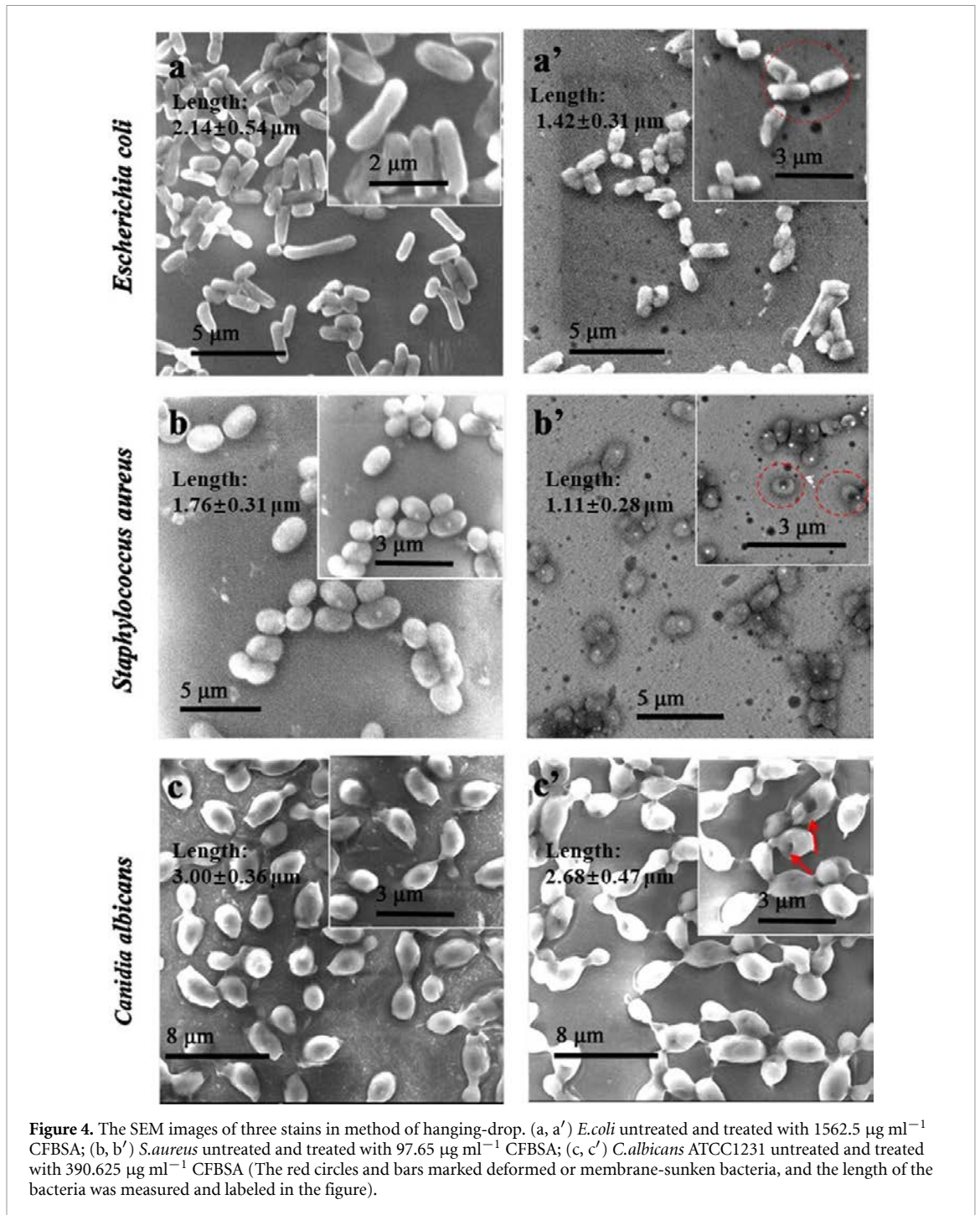
### 4.3. The cytotoxicity

Cytotoxicity is one of the most important evaluation criterions about active drug candidates. Figure 3 showed the cytotoxicity in vitro of compound CFBSA against L929 cells. The MTT results demonstrated CFBSA and NFH had rather low cytotoxicity to L929 cells, and  $\text{IC}_{50}$  value was  $514.3 \pm 33.6 \mu\text{g mL}^{-1}$  and  $398.4 \pm 24.0 \mu\text{g mL}^{-1}$  respectively, indicating the satisfactory cytotoxicity of CFBSA [34]. In conclusion, CFBSA proved to have good antimicrobial activity and low cytotoxicity, manifesting the designed structure of CFBSA contributed to favorable properties. These results may indicate Introduction of fluorine atom seems improve antimicrobial activity

and decrease cytotoxicity. CFBSA was expected to be a novel antimicrobial agent and have further application.

### 4.4. The microorganism morphology

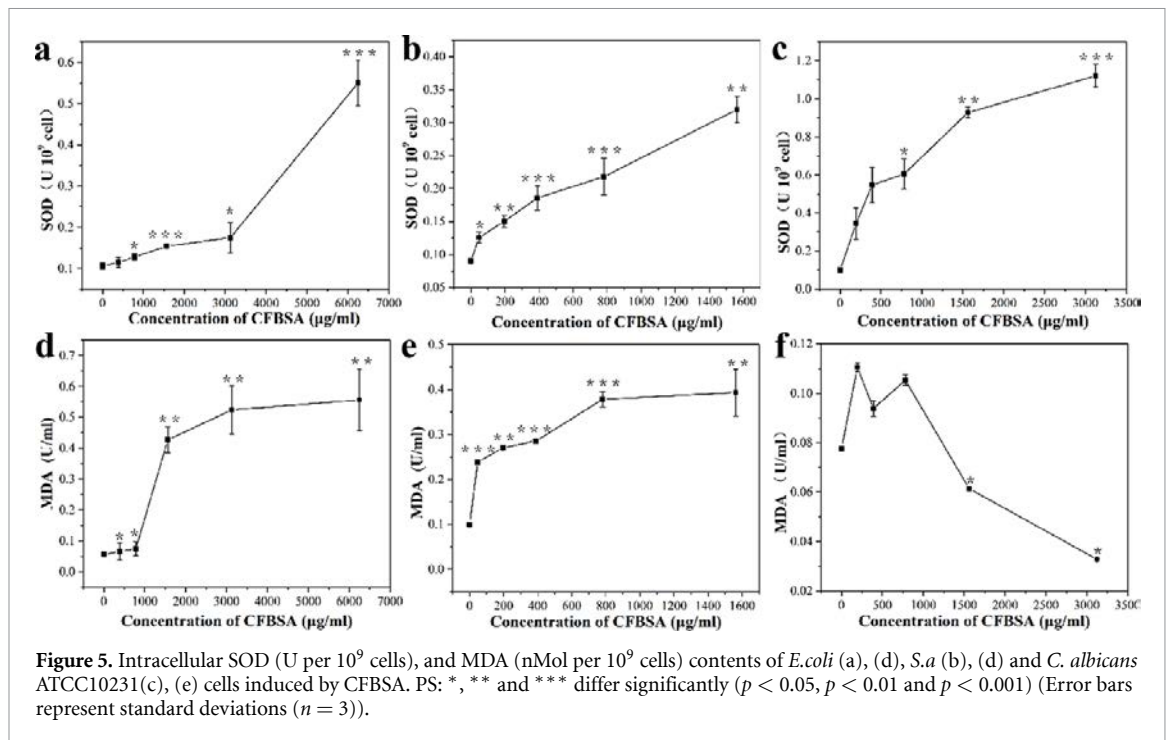
Typical SEM images of the bacterial/fungal untreated and treated with the half MIC concentration of CFBSA are shown in figure 4. The untreated cells of kept normal physiological morphology and unaltered structure. However, the diameter of all microorganisms was significantly reduced after treatment ( $P < 0.5$ ). Obviously, the *E.coli* treated with was  $1562.5 \mu\text{g mL}^{-1}$  CFBSA for 24 h has changed on surface morphology and length (figure 4(a')). It suggested that cell membrane of *E.coli* might be disrupted. As for *S.aureus*, some membrane-sunken cells were noticed from the image of the hanging-drop high concentration treated with  $97.65 \mu\text{g mL}^{-1}$  CFBSA (figure 4(b')). It indicated that CFBSA influenced cell membrane of *S.aureus*. Similarly, the sunken cell membrane arisen on *C.albicans* ATCC1231 (figure 4(c')) after treating with  $390.625 \mu\text{g mL}^{-1}$  CFBSA. It also meant that the compound had an effect on cell membrane of *C.albicans*. Above all, CFBSA probably had a target on cell membrane and killed microorganism by disrupting its cell membrane. However, the hypothesis needs to be confirmed in the expression level or other levels.



#### 4.5. Influence on the oxidative stress

Hence CFBSA is a compound with strong oxidizing properties, influences on the oxidative stress of microorganism caused by CFBSA were determined. MDA is one of the most important products of membrane lipid peroxidation [31]. SOD is an important antioxidant enzyme which is the first position of defense against oxidation [32]. The exposure to CFBSA damaged the antioxidative system and added the oxidative stress on the bacteria, as revealed by the dose-dependent rising of intracellular MDA, and SOD contents (figure 5). Interestingly, with concentration of CFBSA increasing, the MDA

content of treated *C.albicans* ATCC1231 showed a decreased tendency. As reported, the main composition of fungi cell membrane is ergosterol [35], so the MDA content of treated *C.albicans* will not increase. Besides, excess free radicals from CFBSA might oxidize MDA, resulting in MDA content decreasing finally. These findings in according with results of microorganism morphology may reveal the antimicrobial mechanism of CFBSA. It may take oxidative effect on membrane, interrupt the membrane, and kill the bacteria finally. The mechanism needs further confirming in the expression level.



#### 4.6. Surface characterizations of CFBSA loaded PLCL/SF nanofiber

CFBSA loaded PLCL/SF nanofibrous mat was obtained without any bead formation via blend electrospinning. CFBSA proved to be easily dissolved in aprotic solvent (such as HFIP or dichloromethane) and preserve stable [6]. That was the reason why the HFIP was chosen as the only solvent in the blend PLCL/SF electrospinning process. Later, PLCL/SF nanofibrous mats which were loaded with 1%, 2.5%, 5% and 10%(v/v) CFBSA were obtained, and were named SP-1, SP-2.5, SP-5 and SP-10 respectively. Besides, pure PLCL/SF nanofibrous mat was set as positive control in the subsequent experiment and named PSP.

SEM images of PSP, SP-1, SP-2.5, SP-5 and SP-10 were shown in figure 6. It can be directly observed that the surfaces of these blend fibers were smooth, continuous, and bead-less, with no drug crystals forming. As is shown in figures 6(a)–(e), the mean diameter of CFBSA loaded PLCL/SF nanofiber was smaller than the nanofiber with no drug loading. This indicated that when CFBSA was capsuled in PLCL/SF nanofiber. What is more, with the increase of drug loading concentration, the fiber diameter decreases from  $812 \pm 245$  nm to  $526 \pm 120$  nm (figures 6(b)–(c)). This may be because the increase of the ratio of CFBSA which is a polar molecule in the spinning solution raises the charges on the fibers, which increases the electrostatic repulsion force on the fibers during spinning and consequently decreases the diameter of the fibers [8].

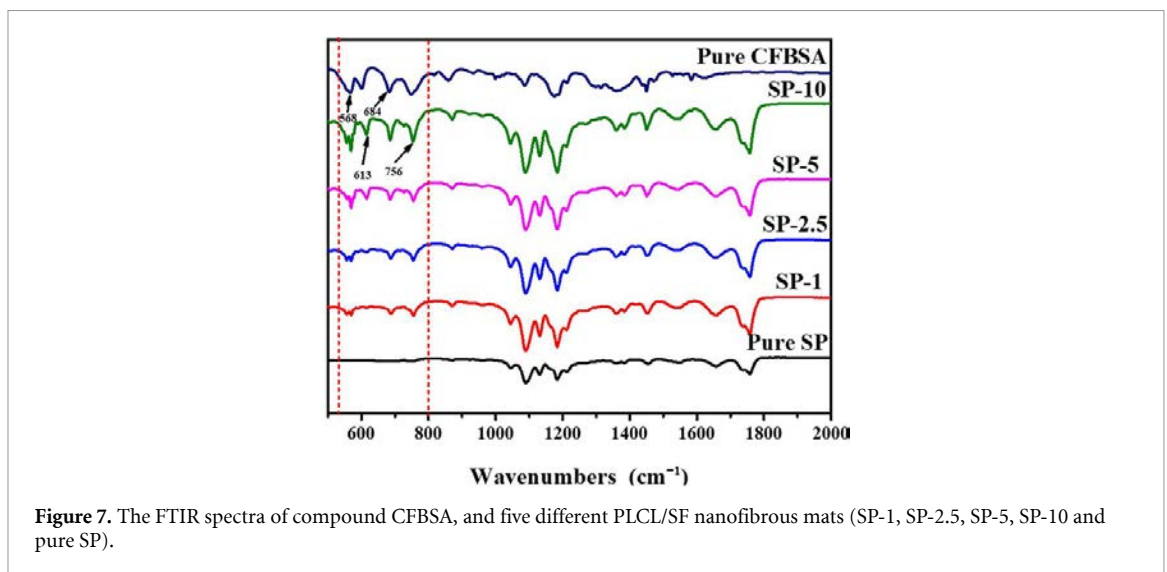
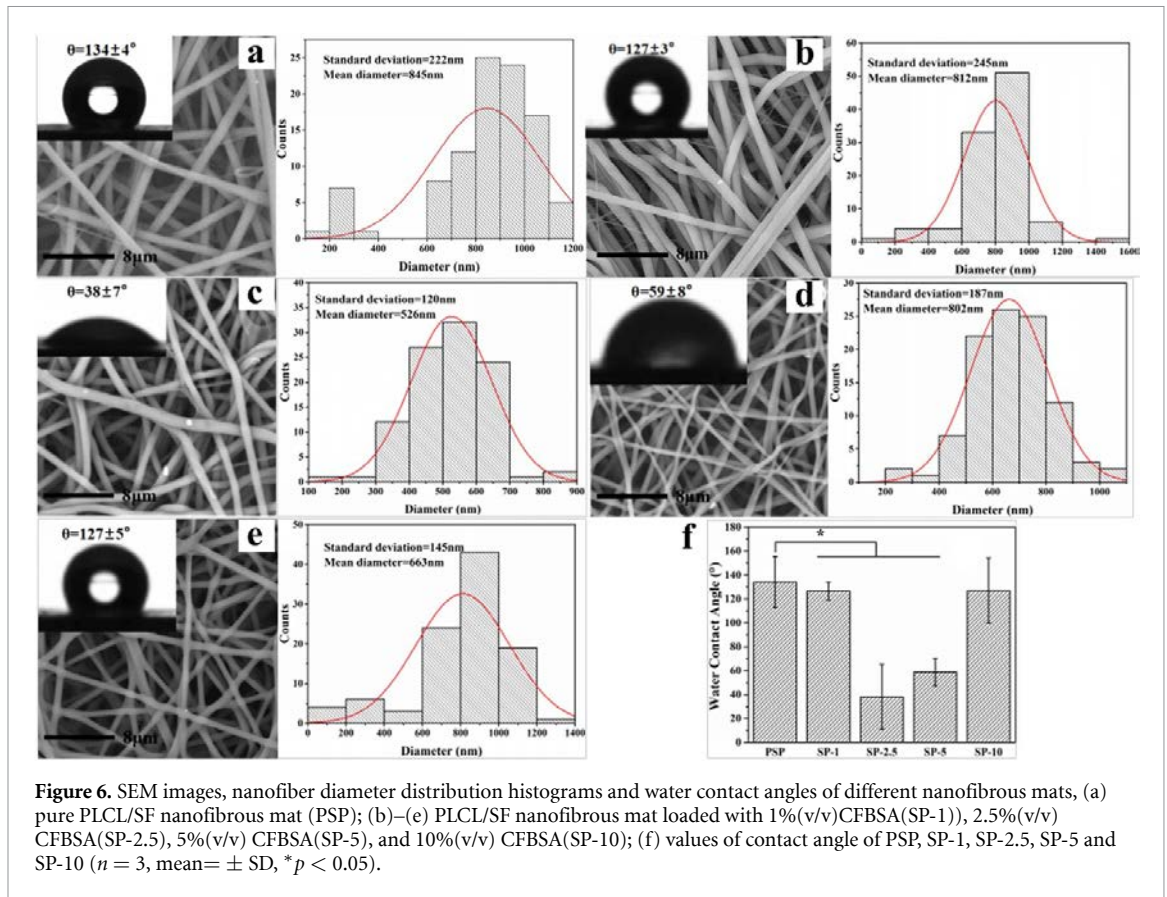
The wetting environment can promote the healing of wounds, and that is the reason why lots of hydrophilic materials were used in the dressings on

the market. As is shown in figures 6(a)–(e), the water contact angle measurement data reflected surface hydrophilicity of these five different nanofibrous mats. There was a clear difference between PSP and SP-1 by contrasting the contact angle values in figure 5(f). It suggested that when the ratio of CFBSA was low, the CFBSA can reduce hydrophobicity of PLCL/SF. Additionally, the value of SP-2.5 and SP-5 had significant difference with PSP, indicating that CFBSA probably changed the intrinsic hydrophobicity of PLCL/SF (figure 6(f)). What is interesting, the contact angle of SP-10 was  $127 \pm 5^\circ$ , which was minor than PSP ( $134 \pm 4^\circ$ ) but bigger than SP-5 ( $59 \pm 8^\circ$ ). It manifested that when the ratio of CFBSA in the spinning solution was enough high, the CFBSA loaded nanofibrous mat exhibited hydrophobic.

It may be that fluorinated compounds (CFBSA) owes low surface energy, which reduces the surface free energy of PLCL/SF nanofibrous mat and makes the material hydrophobic again. Above all, the ratio of CFBSA can directly affect the contact angle of the nanofibrous mat and determine its hydrophobicity or hydrophilicity.

#### 4.7. FTIR spectrum analysis

Infrared spectroscopy is an effective tool for investigating molecular interactions and protein conformation transitions and differing functional groups of compounds. Conformation of silk fibroin the transition can be reflected by the position and intensity of the phthalocyanine peaks, and the conformation of silk fibroin should be random coils, indicating its  $\beta$ -folded conformation. According to the literature, the characteristic absorption peaks of SF are in  $1650\text{--}1660\text{ cm}^{-1}$  (phthalamine I),  $1535\text{--}1545\text{ cm}^{-1}$

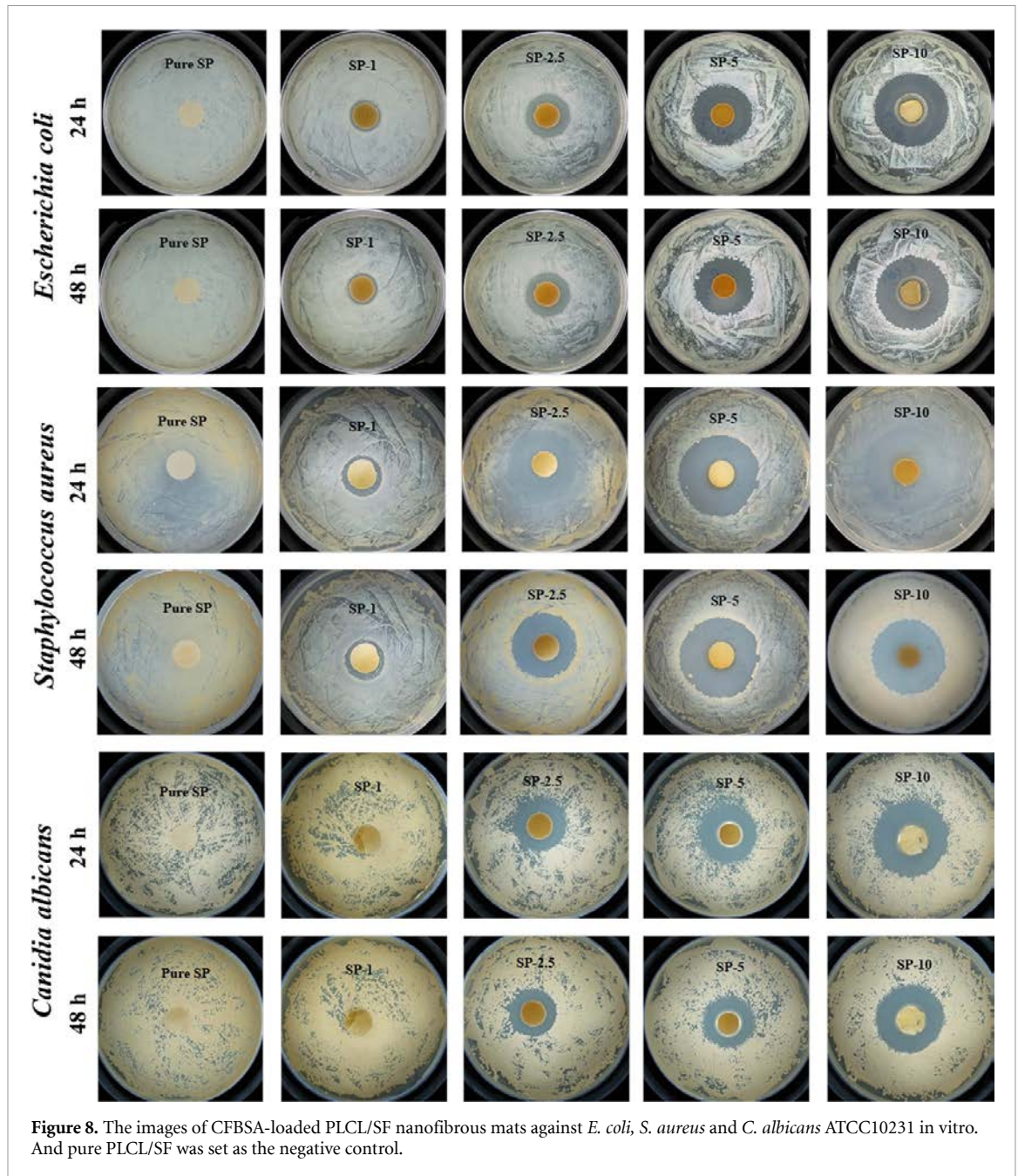


(phthalamine II),  $1235\text{--}1240\text{ cm}^{-1}$  and  $669\text{ cm}^{-1}$  (acid amine V), suggesting the conformation of silk fibroin is mainly random coil. And the characteristic absorption peak of silk fibroin is  $1625\text{--}1640\text{ cm}^{-1}$ ,  $1515\text{--}1525\text{ cm}^{-1}$ ,  $1265\text{ cm}^{-1}$  and  $696\text{ cm}^{-1}$  showed that the conformation of silk fibroin was mainly. It can be observed in figure 7 that there are four characteristic absorption peaks between  $550\text{ cm}^{-1}$  and  $750\text{ cm}^{-1}$  in spectra compound CFBSA and other CFBSA-loaded PLCL/SF mats, while these peaks do not appear on spectra of pure PLCL/SF mat (Pure SP).

Besides, with the increasing ratio of CFBSA (from SP-1 to SP-10), these four characteristic absorption peaks become more sharper, which shows the compound CFBSA was loaded on PLCL/SF successfully and effectively.

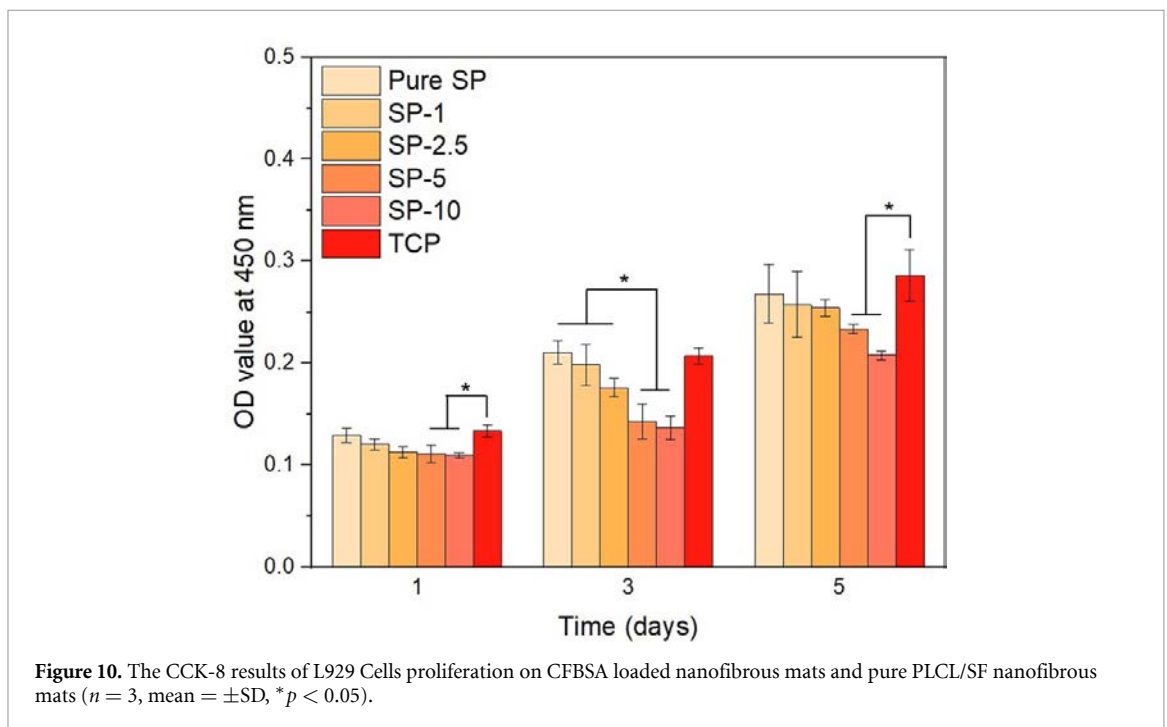
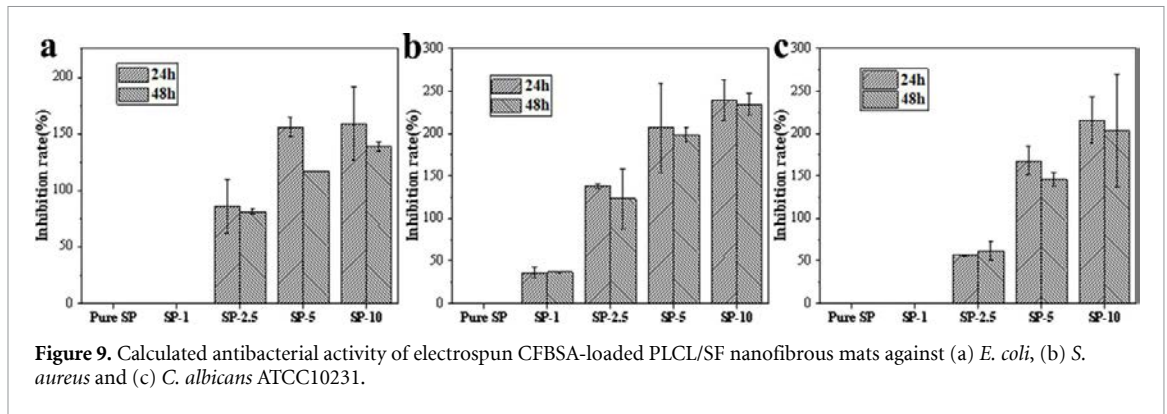
#### 4.8. Antimicrobial assessment of CFBSA loaded nanofibrous mat

The antimicrobial effect of the CFBSA-loaded PLCL/SF nanofibrous mats was assessed by seeding *E. coli* (gram-negative), *S. aureus* (gram-positive) or *C.*



*albicans* (fungi) on these membranes. Photographs of the bacterial and fungal colonies after culturing for 24 h and 48 h at 37 °C are shown in figure 8. As same as previously reported, pure PLCL/SF was found to have no inhibition zone in results of antimicrobial test [12]. On the contrary, this silk fibroin (SF) based material contributed to bacterium attachment and growth, which was attributed to some characteristic of silk fibroin as mentioned above. However, with the increasing ratio of CFBSA, a sharp antimicrobial activity of CFBSA-loaded PLCL/SF membranes could be observed in figure 8. As is shown in figure 9(a), inhibition rate of SP-2.5 against *E. coli* was  $56.6 \pm 0.9\%$ , and its inhibition rate against *S. aureus* and *C. albicans* were  $85.8 \pm 5.0\%$  and  $138.7 \pm 1.7\%$  (figures 9(a) and (b)). Inhibition rates of SP-5 against *E. coli*, *S. aureus* and *C. albicans* were

$168.0 \pm 4.0\%$ ,  $207.0 \pm 7.3\%$  and  $156 \pm 3.0\%$  respectively (figures 9(a)–(c)), which showed excellent antimicrobial activity of SP-2.5. As for SP-10, its inhibition rate against *E. coli*, *S. aureus* and *C. albicans* could reach  $216.1 \pm 5.2\%$ ,  $239.0 \pm 4.9\%$  and  $159 \pm 5.7\%$  separately, indicating SP-10 antimicrobial activity. Additionally, there were no evident differences the results between 24 h and 48 h ( $P > 0.05$ ), suggesting the wide-broad bactericidal of CFBSA-loaded mats. However, SP-1 seemed to have inhibition area against *S. aureus*, simply, while its inhibition rate of 24 h was  $19.3 \pm 5.6\%$ . This may indicate that the ratio of CFBSA loaded on mats and antimicrobial activity were dose effect dependency relationship, and the effective dose of CFBSA in PLCL/SF fibrous mat against most pathogenic bacteria was over 2.5(v/v).



In conclusion, CFBSA-loaded PLCL/SF fibrous mat showed predominant antimicrobial and bactericidal activity of against gram-positive, gram-negative bacteria and fungi. It should be attributed to the CFBSA drug released from the nanofiber mat. Especially SP-2.5, SP-5 and SP-10 exhibited evident inhibition areas against three different types of strains, indicating CFBSA improved antimicrobial activity of PLCL/SF fibrous mat and its potential application for antibiotic wound dressing.

Antimicrobial activity related to membrane permeability has been extensively studied in the literature [35–37]. As a gram-positive bacterium, the cell membrane of *S. aureus* is not thick enough to defend oxidation from CFBSA, and that may be the reason why CFBSA and CFBSA-loaded PLCL/SF have better antibacterial activity for *S. aureus* than against *E. coli* (gram-negative bacteria) in this test. The different antimicrobial efficiencies among three strains could also prove some hypothesis about antibacterial mechanisms of CFBSA in previous study.

#### 4.9. L929 cells proliferation on CFBSA loaded nanofibrous mat

Biocompatibility is a vital factor in biomedical applications, so it is essential to examine the biocompatibility of the CFBSA loaded nanofibrous materials. Cell proliferation *in vitro* was measured by using a CCK-8 assay of L929 cells on different CFBSA-loaded electrospun PLCL/SF fibrous mats, and the pure nanofibrous mat was evaluated together with tissue culture plate (TCP) as control. As is showed in figure 10, the L929 cells of each group proliferated sequentially from 1 d to 5 d after culturing in 24 well plate. It declared that CFBSA-loaded PLCL/SF fibrous mats had good biocompatibility, which was consisted with the results of cytotoxicity *in vitro* of compound CFBSA. Notably, the L929 cells proliferation behavior on pure PLCL/SF group did not differ from that on the TCP group ( $P < 0.05$ ), this phenomenon proved the results in report above in the introduction [15]. However, after loaded with different concentration of CFBSA, there was significant differences among the

SP-5, SP-10 and TCP at days 1 and 5 ( $P < 0.05$ ). At day 3, although SP-5, SP-10 were not significantly different from the TCP group, they were significantly different from the other three groups ( $P < 0.05$ ). It was suggested that when the ratio of CFBSA in the electrospinning solution was over 5%, the developed nanofibrous mat showed a negative effect on proliferation of L929 cells. Thus, when the ratio of CFBSA in the spinning solution was no more than 2.5%, the fabricated CFBSA-loaded PLCL/SF nanofibrous mats had no cytotoxicity or negative influences on the proliferation of L929 cells and was always biocompatible. In addition, the results antimicrobial assessment in vitro also demonstrated that SP-2.5 possessed antimicrobial performance and prevented bacterial biofilm formation effectively. Therefore, the ratio of CFBSA in SP-2.5 may be regarded as a worthwhile reference to the further application of CFBSA-loaded PLCL/SF.

## 5. Conclusion

In summary, compound CFBSA was firstly proved as a wide-broad antimicrobial and bactericidal drug against different gram-negative bacteria, gram-positive bacteria, and fungi, while it was identified to have low cytotoxicity and its  $IC_{50}$  was  $514.3 \pm 33.6 \mu\text{g ml}^{-1}$ . It seems that introduction of fluorine atom has improved antimicrobial activity and decrease cytotoxicity, suggesting the reasonable design of CFBSA. Identifying by morphology observation and measurement of the oxidative stress on cells, CFBSA proved to have effect on membrane of bacteria and fungi. This could be the reason why it has broad-spectrum antimicrobial activity. Due to strong bactericidal effect of CFBSA, it is not easy to induce the production of drug-resistant bacteria. CFBSA may be regarded as a wide-broad bactericidal drug, and it is expected to be applied in wound dressing.

Different concentrations of CFBSA were loading on PLCL/SF nanofibrous mats via electrospinning successfully, which performed potential application in wound dressing. The CFBSA-loaded PLCL/SF nanofibrous mats exhibited variant diameter distribution histograms and water contact angles depended on the ratio of CFBSA. Notably, all the CFBSA-loaded PLCL/SF fibrous mats exerted favorable antimicrobial activity and SP-2.5, SP-5, SP-10 owed significant antibacterial effects against *S. aureus*, *E. coli* and *C. albicans*. And the biocompatibility of CFBSA-loaded PLCL/SF mats was confirmed that when the ratio of CFBSA in the spinning solution was no more than 2.5% (v/v), the fabricated CFBSA-loaded PLCL/SF nanofibrous mat had no cytotoxicity for L929 cells. Concerned about biocompatibility and antibacterial efficiency, SP-2.5 was chosen as the ideal CFBSA-loaded concentration for the further application of CFBSA-loaded PLCL/SF. In addition, the results antimicrobial assessment in vitro also demonstrated that SP-2.5 possessed antimicrobial

performance and prevented bacterial biofilm formation effectively. Therefore, the ratio of CFBSA in SP-2.5 may be regarded as a worthwhile reference to the further application of CFBSA-loaded PLCL/SF. In short, due to its low toxicity and excellent broad-spectrum antimicrobial properties, CFBSA will certainly have a great future in antibacterial industry.

## Data availability statement

All data that support the findings of this study are included within the article (and any supplementary files).

## Acknowledgments

This work was supported by the Fundamental Research Funds for the Central Universities (No.2232023D-10). This project was also supported by Researchers Supporting Project Number (RSP2024R65), King Saud University, Riyadh, Saudi Arabia.

## Conflict of interest

There are no conflicts to declare.

## ORCID iDs

Shu Sun  <https://orcid.org/0009-0007-3420-8677>

Jinglei Wu  <https://orcid.org/0000-0001-9549-3992>

Mohamed El-Newehy  <https://orcid.org/0000-0002-4265-0701>

Hao Zheng  <https://orcid.org/0009-0002-8108-5044>

## References

- [1] Gaynes R 2017 The discovery of penicillin—new insights after more than 75 years of clinical use *Emerg. Infect. Dis. J.* **23** 849
- [2] Davies J 1996 Origins and evolution of antibiotic resistance *Microbiologia* **12** 9–16
- [3] Azucena E and Mobashery S 2001 Aminoglycoside-modifying enzymes: mechanisms of catalytic processes and inhibition *Drug Resist. Updat.* **4** 106–17
- [4] Zhao F, Wang J, Ding X, Shu S and Liu H 2016 Application of sulfonyl in drug design *Chin. J. Org. Chem.* **36** 490
- [5] Muller K, Faeh C and Diederich F 2007 Fluorine in pharmaceuticals: looking beyond intuition *Science* **317** 1881–6
- [6] Pu X Q, Zhao H-Y, Lu Z-H, He X-P and Yang X-J 2016 Aminochlorination of Alkenes with CFBSA *Eur. J. Org. Chem.* **2016** 4526–33
- [7] Jiang P-P and Yang X-J 2016 A quick, mild and efficient bromination using a CFBSA/KBr system *RSC Adv.* **6** 90031–4
- [8] Lu Z, Li Q, Tang M, Jiang P, Zheng H and Yang X 2015 CFBSA: a novel and practical chlorinating reagent *Chem. Commun.* **51** 14852–5
- [9] Sen C K, Gordillo G M, Roy S, Kirsner R, Lambert L, Hunt T K, Gottrup F, Gurtner G C and Longaker M T 2009 Human skin wounds: a major and snowballing threat to

- public health and the economy *Wound Repair Regen.* **17** 763–71
- [10] Mensah A Y, Houghton P J, Dickson R A, Fleischer T C, Heinrich M and Bremner P 2006 In vitro evaluation of effects of two Ghanaian plants relevant to wound healing *Phytother. Res.* **20** 941–4
- [11] Inngjerdingen K, Nergård C S, Diallo D, Mounkoro P P and Paulsen B S 2004 An ethnopharmacological survey of plants used for wound healing in Dogonland, Mali, West Africa *J. Ethnopharmacol.* **92** 233–44
- [12] Kim S-H, Kwon J H, Chung M S, Chung E, Jung Y, Kim S H and Kim Y H 2006 Fabrication of a new tubular fibrous PLCL scaffold for vascular tissue engineering *J. Biomater. Sci. Polym. Ed.* **17** 1359–74
- [13] Yan S, Xiaoqiang L, Lianjiang T, Chen H and Xiumei M 2009 Poly (l-lactide-co- $\epsilon$ -caprolactone) electrospun nanofibers for encapsulating and sustained releasing proteins *Polymer* **50** 4212–9
- [14] Zhang K, Wang H, Huang C, Su Y, Mo X and Ikada Y 2010 Fabrication of silk fibroin blended P (LLA-CL) nanofibrous scaffolds for tissue engineering *J. Biomed. Mater. Res. A* **93** 984–93
- [15] Zhang K, Yin A, Huang C, Wang C, Mo X, Al-Deyab S S and El-Newehy M 2011 Degradation of electrospun SF/P (LLA-CL) blended nanofibrous scaffolds in vitro *Polym. Degrad. Stab.* **96** 2266–75
- [16] Kaur J, Rajkhowa R, Afrin T, Tsuzuki T and Wang X 2014 Facts and myths of antibacterial properties of silk *Biopolymers* **101** 237–45
- [17] Maharjan B, Joshi M K, Tiwari A P, Park C H and Kim C S 2017 In-situ synthesis of AgNPs in the natural/synthetic hybrid nanofibrous scaffolds: fabrication, characterization and antimicrobial activities *J. Mech. Behav. Biomed. Mater.* **65** 66–76
- [18] Shi R, Geng H, Gong M, Ye J, Wu C, Hu X and Zhang L 2018 Long-acting and broad-spectrum antimicrobial electrospun poly ( $\epsilon$ -caprolactone)/gelatin micro/nanofibers for wound dressing *J. Colloid Interface Sci.* **509** 275–84
- [19] Zhang W, Ronca S and Mele E 2017 Electrospun nanofibres containing antimicrobial plant extracts *Nanomaterials* **7** 42
- [20] Xu H, Fang Z, Tian W, Wang Y, Ye Q, Zhang L and Cai J 2018 Green fabrication of amphiphilic quaternized  $\beta$ -chitin derivatives with excellent biocompatibility and antibacterial activities for wound healing *Adv. Mater.* **30** 1801100
- [21] Mooney E K, Lippitt C and Friedman J 2006 Silver dressings *Plast. Reconstr. Surg.* **117** 666–9
- [22] Qin J, Guo J, Xu Q, Zheng Z, Mao H and Yan F 2017 Synthesis of pyrrolidinium-type poly (ionic liquid) membranes for antibacterial applications *ACS Appl. Mater. Interfaces* **9** 10504–11
- [23] Atiyeh B S, Costagliola M, Hayek S N and Dibo S A 2007 Effect of silver on burn wound infection control and healing: review of the literature *Burns* **33** 139–48
- [24] Wong K K Y and Liu X 2010 Silver nanoparticles—the real “silver bullet” in clinical medicine? *MedChemComm* **1** 125–31
- [25] Park M V D Z, Neigh A M, Vermeulen J P, de la Fonteyne L J J, Verharen H W, Briedé J J, van Loveren H and de Jong W H 2011 The effect of particle size on the cytotoxicity, inflammation, developmental toxicity and genotoxicity of silver nanoparticles *Biomaterials* **32** 9810–7
- [26] Morar M and Wright G D 2010 The genomic enzymology of antibiotic resistance *Annu. Rev. Genet.* **44** 25–51
- [27] Heyneman A, Hoeksema H, Vandekerckhove D, Pirayesh A and Monstrey S 2016 The role of silver sulphadiazine in the conservative treatment of partial thickness burn wounds: a systematic review *Burns* **42** 1377–86
- [28] Lin Y et al 2023 Discovery of new broad-spectrum anti-infectives for eukaryotic pathogens using bioorganometallic chemistry *J. Med. Chem.* **66** 15867–82
- [29] Jin C, Kaewintajuk K, Jiang J, Jeong W, Kamata M, KIM H-S, Wataya Y and Park H 2009 Toxoplasma gondii: a simple high-throughput assay for drug screening in vitro *Exp. Parasitol.* **121** 132–6
- [30] Gönenç A, Ozkan Y, Torun M and Simsek B 2001 Plasma malondialdehyde (MDA) levels in breast and lung cancer patients *J. Clin. Pharm. Ther.* **26** 141–4
- [31] Yin Y, Han W and Cao Y 2019 Association between activities of SOD, MDA and Na<sup>+</sup>-K<sup>+</sup>-ATPase in peripheral blood of patients with acute myocardial infarction and the complication of varying degrees of arrhythmia *Hell. J. Cardiol.* **60** 366–71
- [32] Jain S K 1989 Hyperglycemia can cause membrane lipid peroxidation and osmotic fragility in human red blood cells *J. Biol. Chem.* **264** 21340–5
- [33] Chiou J-F and Hu M-L 1999 Elevated lipid peroxidation and disturbed antioxidant enzyme activities in plasma and erythrocytes of patients with uterine cervicitis and myoma *Clin. Biochem.* **32** 189–92
- [34] Gao E, Sun N, Zhang S, Ding Y, Qiu X, Zhan Y and Zhu M 2016 Synthesis, structures, molecular docking, cytotoxicity and bioimaging studies of two novel Zn (II) complexes *Eur. J. Med. Chem.* **121** 1–11
- [35] Lee M-W, Park S C, Chae H-S, Bach J-H, Lee H-J, Lee S H, Kang Y K, Kim K Y, Lee W B and Kim S S 2001 The protective role of HSP90 against 3-hydroxykynurenine-induced neuronal apoptosis *Biochem. Biophys. Res. Commun.* **284** 261–7
- [36] Cowen L E 2008 The evolution of fungal drug resistance: modulating the trajectory from genotype to phenotype *Nat. Rev. Microbiol.* **6** 187–98
- [37] Zhao R et al 2005 Navigating the chaperone network: an integrative map of physical and genetic interactions mediated by the hsp90 chaperone *Cell* **120** 715–27